SF2A 2016
C. Reylé, J. Richard, L. Cambrésy, M. Deleuil, E. Pécontal, L. Tresse and I. Vauglin (eds)

EVOLUTION OF SOLIDS IN THE JOVIAN SUBNEBULA: IMPLICATIONS FOR THE FORMATION OF THE GALILEAN SATELLITES

T. Ronnet[1], O. Mousis[1] and P. Vernazza[1]

Abstract. The four Galilean satellites are thought to have formed within an accretion disk surrounding Jupiter during the late stages of its formation. Here we investigate the fate of solids of different sizes in the accretion disk. The dynamics of the solids is followed along with their thermodynamic evolution. This allows us to track the water ice-to-rock mass fraction of the planetesimals as they sublimate and lose mass when heated in the disk. We then compare our results to the known bulk composition of the Jovian moons and draw some conclusions as regards their formation.

Keywords: Galilean satellites, formation, pebbles, accretion disk

1 Introduction

During the late stages of giant planets formation, the gas accreted onto the envelope of the planet must proceed through an accretion disk because of its high angular momentum preventing it to be directly accreted onto the surface of the planet. This process has been illustrated in several studies based on 3D hydrodynamic (e.g, Klahr & Kley 2006; Tanigawa et al. 2012; Szulágyi et al. 2016) and magneto-hydrodynamic (Gressel et al. 2013) simulations. There is little doubt the four Galilean satellites, Io, Europa, Ganymede and Callisto, formed within such a disk surrounding Jupiter in the very end of its formation. The structure of the circumplanetary disk (CPD) however, also called a subnebula, and the size and origin of the solids that eventually formed the satellites, are yet to be constrained. There are currently two main scenarios for the formation of the Jovian moons, one based on a minimum mass subnebula (Mosqueira & Estrada 2003a,b) where all the mass in solids required for forming the satellites is present at one time, and an other one based on an actively-supplied subnebula (Canup & Ward 2002), referred to as the gas-starved disk model, where solids are constantly brought from the surrounding nebula to the sebnubela via the infalling gas flow.

Here we present a lagrangian integrator we developed to track solids evolution within the subnebula of Jupiter. We study planetesimals with a large range of sizes, from 10^{-6} up to 10^{6} m. The dynamic of the solids is affected by aerodynamic drag due to their relative velocity with the gas and by turbulent diffusion. The evolution of the surface temperature is also computed and allows us to determine the mass ablation rate of the bodies and to follow their ice-to-rock mass fraction accordingly.

The subnebula and solids evolution models are further exposed in the next section, while some results are presented in section 3.

2 Models

2.1 Subnebula model

The subnebula model derived in Canup & Ward (2002) is a more physically motivated model than minimum mass models which is why we favored it in this study. In this actively supplied accretion disk, or gas starved disk, the repartition of gas in the subnebula is given by considering a balance between the infall of material from the nebula to the CPD and the accretion onto the surface of Jupiter from the CPD. The gas is equally reparted from the inner edge of the disk to the centrifugal radius r_c, the distance where the gravitational potential of the

[1] Aix Marseille Univ, CNRS, LAM, Laboratoire d'Astrophysique de Marseille, Marseille, France

central planet balances the angular momentum of the infalling material. Though the position of the centrifugal radius should evolve with time, being farther and farther from Jupiter as the forming planet's mass increases, here we are interested in the very late stages of Jupiter formation. In our model, the mass of the central planet is therefore $1\,M_{\rm Jup}$ and the centrifugal radius is fixed at $26\,R_{\rm Jup}$ while the outer disk edge is placed at $r_d = 150\,R_{\rm Jup}$. The surface density of the gas is then given by:

$$\Sigma_g(r) = \frac{\dot{M}_p}{3\pi\nu} \begin{cases} 1 - \frac{4}{5}\sqrt{\frac{r_c}{r_d}} - \frac{1}{5}\left(\frac{r}{r_c}\right)^2 & \text{for } r \leqslant r_c, \\ \\ \frac{4}{5}\sqrt{\frac{r_c}{r}} - \frac{4}{5}\sqrt{\frac{r_c}{r_d}} & \text{for } r > r_c. \end{cases} \tag{2.1}$$

In the above expression, $\dot{M}_p$ is the mass accretion rate onto Jupiter, which is also the mass accretion rate from the nebula to the CPD, $\nu = \alpha H_g^2 \Omega_K$ is the effective turbulent viscosity, with Ω_K the keplerian orbital frequency and H_g is the gas scale height calculated from the vertical hydrostatic equilibrium of the gas with an isothermal equation of state $P = c_g^2 \rho_g$, and $c_g^2 = R_g T_d/\mu$. The molecular weight of the gas is $\mu = 2.4\,{\rm g\,mol^{-1}}$ and the temperature distribution in the subnebula is taken from the simple prescription of Sasaki et al. (2010) which gives

$$T_d \simeq 225 \left(\frac{r}{10\,R_{\rm Jup}}\right)^{3/4} \left(\frac{\dot{M}_p}{10^{-7}\,M_{\rm Jup}\,{\rm yr^{-1}}}\right)^{1/4} {\rm K}. \tag{2.2}$$

2.2 Gas dynamics

Here we are interested in the evolution of solids within the subnebula, whose dynamic is affected by interaction with the gas through friction forces. In order to determine these, we need to calculate the velocity of the gas in the disk.

The most important velocity to determine is actually the azimuthal velocity. Because of the pressure force arising from the density gradient within the disk, the gas rotates at a slightly subkeplerian velocity with a deviation given by

$$v_{\phi,g} \equiv v_K - \eta v_K \approx v_K + \frac{1}{2}\frac{c_g^2}{v_K}\frac{\partial \ln P}{\partial \ln r}\,. \tag{2.3}$$

The keplerian velocity is $v_K = r\Omega_K$ with $\Omega_K = \sqrt{GM_p}/r^3$. Because solids do not feel this pressure force, they would rotate at a slightly higher velocity than the gas and feel a headwind that causes their orbit to decay. Solids dynamics is presented in more details in the next section. It is important to note that the gas rotates at a subkeplerian velocity in the general case of the inward pressure gradient, i.e. outward pressure force opposed to the gravitational attraction of the central planet, but that an outward pressure gradient, such as that created at the outer edge of a gap opened by a planet in a proto-planetary disk (PPD), would result in a gas rotating at a superkeplerian velocity.

We assume that the gas is in hydrostatic equilibrium in the vertical direction and its vertical velocity is therefore zero. Although this is not exactly accurate, the assumption is valid as demonstrated by Keller & Gail (2004) and Takeuchi & Lin (2002). Knowing the vertical and azimuthal velocity of the gas, the radial velocity of the gas can be derived from the azimuthal momentum equation of the viscous gas. We are then able to calculate gas velocity in the CPD in all directions.

2.3 Particles dynamics

The motion of solids within the subnebula is affected by interaction with the gas in two different ways. Firstly, solids motion is affected by friction forces due to their relative velocity with the gas. The friction force is expressed through the stopping time t_s of the particle, which contains all the physics of the interaction with the gas. It is separated in two regimes, one where the particle size is much smaller than the mean free path of molecules in the gas and the stopping time does depend on the relative velocity between the gas and the particle, referred to as the Epstein regime, and another one where gas should be regarded as a fluid and the stopping time of the particle depends on its relative velocity with respect with the gas:

$$t_s = \left(\frac{\rho_g v_{th}}{\rho_s R_s} \min\left[1, \frac{3}{8}\frac{v_{rel}}{v_{th}} C_D(Re)\right]\right)^{-1}. \tag{2.4}$$

This stopping time is the characteristic time of angular momentum exchange between the gas and the particle. The drag coefficient C_D is a dimensionless quantity that depends upon the Reynolds number of the flow around the particle.

From this, particles velocity is obtained by numerically integrating their equation of motion. The equation is integrated with an adaptive timestep ODE solver (Brown et al. 1989), using Adams methods for particles with sizes down to 10^{-3} m, while an implicit backward differentiation formula scheme is used to integrate the motion of smaller particles whose small stopping times imply a too restrictive timestep for the Adams methods.

The second effect affecting solids motion is turbulence within the CPD. Turbulent eddies are able to entrain particles during their cohesion time, which is approximately the inverse of the local keplerian frequency. Finally, turbulence acts as a diffusion mechanism which we model, following Ciesla (2010, 2011) and Charnoz et al. (2011), with a stochastic motion and advection terms arising from gradients in the diffusivity of particles and density of the gas.

2.4 Particles thermodynamics

An interesting feature of our model is that we also implemented solids thermodynamics. In this study, we restricted ourselves to a mixture of silicates and water ice, but different types of ices can easily be implemented.

All solids, regardless of their sizes, start with a ice-to-rock mass fraction of 0.5, representative of bodies formed beyond the water ice line of the solar nebula. The surface temperature of the planetesimals is calculated using heating and cooling energie sources, following D'Angelo & Podolak (2015). The primary source of energy is the radiation from the surrounding gas. Another heating mechanism is the friction with the gas that heats up the surface of planetesimals. The ablation of ice, on the other end, is an endothermal process which tends to cool down the body.

The theoretical maximum ablation rate of water ice at the surface of the body is given by

$$\frac{dMs}{dt} = -4\pi R_s^2 P_v \sqrt{\frac{\mu_s}{2\pi R_g T_s}}. \tag{2.5}$$

Here, P_v is the equilibrium water vapor pressure of water over water ice at the temperature T_s which is taken from Fray & Schmitt (2009). The mass ablation rate can be used also to determine the change in radius of a particle as it ablates.

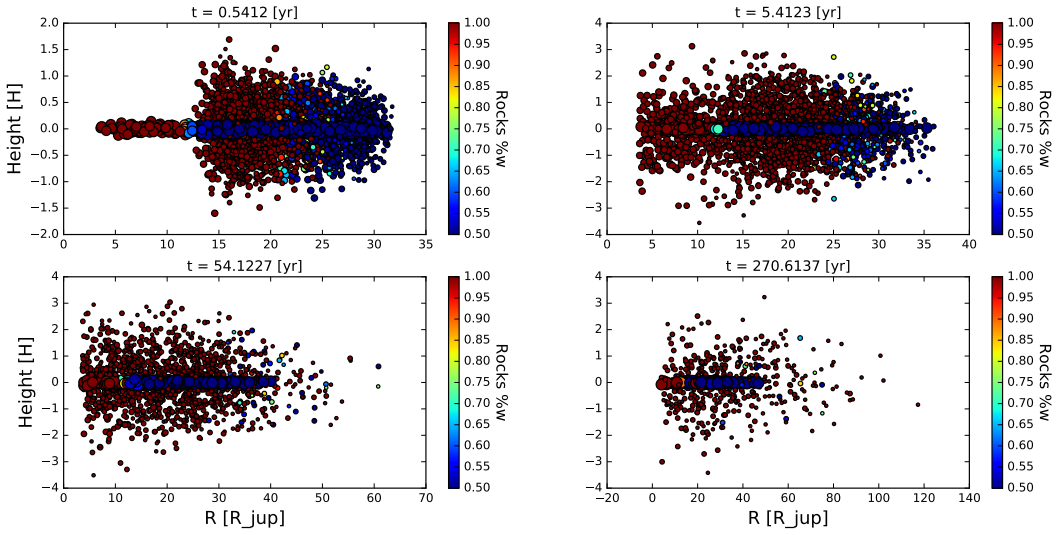

Fig. 1. Simulation of 10^4 particles with initial sizes ranging from 10^{-6} up to 10^6 m. Particles were initially released between 15 and 25 $R_{\rm Jup}$ and all contained 50% of water ice by mass. All particles also started at the midplane of the disk and their vertical distribution is the result of turbulent transport only. Vertical transport proceeds on shorter timescales than radial diffusion as can be seen from the top left panel where particles are size sorted in the vertical direction already.

The temperature evolution, along with the ablation rate, and thus the change in radius, are solved together with the equation of motion of the particle. We are thus able to consistently follow the evolution of the solids in the Jovian subnebula, including for the first time their water ice content.

3 Results

We present in figure 1 an example of simulation with 10^4 particles with sizes ranging 10^{-6}–10^6 m. All particles were initially released between 15 and 30 $R_{\rm Jup}$ at the midplane of the disk with 50% of water ice by mass. The observed vertical distribution of solids is solely due to turbulent stirring of grains. The settling of larger grains to the midplane of the disk is clearly illustrated, although the reading of the figure is not straight, especially because a very wide range of particle size was used and their representation is uneasy. However, some interesting features are observed. The most important one would probably be that solids of different sizes have a different water ice mass fraction at the same location in the disk, which is clearly identifiable in the top left panel of figure 1 corresponding to the very beginning of the simulation. Although after some time a lot of particles are lost from the simulation and turbulence efficiently mixes the smallest grains, it is clear that bigger bodies are able to carry water further inside the disk.

Further investigations of the presented result will certainly help in better constraining the formation of the Galilean satellites. More specifically, to constrain the size of the building blocks of the moons and their origin by comparing with their bulk composition.

References

Brown, P. N., Byrne, G. D., & Hindmarsh, A. C. 1989, SIAM J. Sci. Stat. Comput., 10, 1038
Canup, R. M., & Ward, W. R. 2002, AJ, 124, 3404
Charnoz, S., Fouchet, L., Aleon, J., & Moreira, M. 2011, ApJ, 737, 33
Ciesla, F. J. 2010, ApJ, 723, 514
Ciesla, F. J. 2011, ApJ, 740, 9
D'Angelo, G., & Podolak, M. 2015, ApJ, 806, 203
Dwyer, C. A., Nimmo, F., Ogihara, M., & Ida, S. 2013, Icarus, 225, 390
Fray, N., & Schmitt, B. 2009, Planet. Space Sci., 57, 2053
Gressel, O., Nelson, R. P., Turner, N. J., & Ziegler, U. 2013, ApJ, 779, 59
Keller, C., & Gail, H.-P. 2004, A&A, 415, 1177
Klahr, H., & Kley, W. 2006, A&A, 445, 747
Mosqueira, I., & Estrada, P. R. 2003, Icarus, 163, 198
Mosqueira, I., & Estrada, P. R. 2003, Icarus, 163, 232
Sasaki, T., Stewart, G. R., & Ida, S. 2010, ApJ, 714, 1052
Szulágyi, J., Masset, F., Lega, E., et al. 2016, MNRAS, 460, 2853
Takeuchi, T., & Lin, D. N. C. 2002, ApJ, 581, 1344
Tanigawa, T., Ohtsuki, K., & Machida, M. N. 2012, ApJ, 747, 47